Free energy of bcc iron: Integrated *ab initio* derivation of vibrational, electronic, and magnetic contributions

F. Körmann,[1,*] A. Dick,[1] B. Grabowski,[1] B. Hallstedt,[2] T. Hickel,[1] and J. Neugebauer[1]
[1]*Max-Planck-Institut für Eisenforschung GmbH, Düsseldorf D-40237, Germany*
[2]*Materials Chemistry, RWTH Aachen University, Aachen, Germany*
(Received 10 March 2008; published 3 July 2008)

We present *ab initio* derived thermodynamic properties of ferromagnetic bcc iron up to the bcc-fcc phase-transition temperature (1200 K), including vibrational, electronic, and magnetic contributions. The quasiharmonic approximation and finite-temperature density-functional theory are employed to account for vibrational and electronic excitations. The magnetic contribution is derived from the solution of the quantum Heisenberg model within many-body theory using the mean-field and random-phase approximation. The calculated thermodynamic properties show an excellent agreement with available experimental data and reveal the necessity to consider all three types of excitations.

DOI: 10.1103/PhysRevB.78.033102 PACS number(s): 71.15.−m, 63.20.−e, 75.40.Cx, 75.50.Bb

A key quantity in fully characterizing the thermodynamic properties of materials is the Helmholtz free energy of their individual structural and magnetic phases. Well established simulation tools, e.g., CALPHAD (Refs. 1 and 2), use empirical interpolation formulas and experimental input to describe the temperature dependence of this energy. However, experimental input data, e.g., for novel alloy systems or metastable structures, are not always available. Therefore, there is a strong interest in incorporating *ab initio* results into these simulation tools.[3] Based on density-functional theory (DFT), substantial progress has been made in determining *ab initio* free energies for elementary nonmagnetic materials.[4,5] Here, lattice vibrations and (in particular for transition metals) electronic excitations yield the dominant contributions to the entropy. Despite its great importance for many practical applications (e.g., steel, magnetic actuators), the *ab initio* treatment of the magnetic contribution is discussed to a much less extent. However, only if all relevant excitation processes can be described with a total accuracy of a few meV within an integrated approach, a reliable *ab initio* prediction of thermodynamic properties in these materials can be expected. We have chosen iron as the most prominent magnetic material in order to develop such an integrated computational treatment and to test whether the accuracy of common DFT functionals is sufficient to achieve this goal.

We will concentrate our investigation on the treatment of magnetic properties. In the past, several methods (e.g., a multiband Hubbard model,[6] spin-fluctuation theory,[7,8] the Heisenberg model[9] solved within the Monte Carlo method,[10–13] or many-body theory[11,14,15]) have been used for calculating quantitative temperature-dependent magnetic properties from *ab initio* input. However, most of them focused on the calculation of the magnetization and the Curie temperature. Much less attention is paid to the magnetic free energy, although it is well established that magnetic excitations are of crucial importance for the structural phase stability in iron.[16,17] An existing approach, based on the single-band spin-fluctuation theory within the mean-field approximation, gives a good qualitative agreement with experiment but fails to provide a reasonable quantitative description of the magnetic free energy.[17] In this Brief Report, we, therefore, propose an accurate method for calculating the magnetic free energy using *ab initio* input and many-body theory for the Heisenberg model. We show that the magnetic contribution is essential for the description of thermodynamic properties and, if properly taken into account, allows for a quantitative description over the entire temperature range relevant for the considered phase.

For the present purpose, the Helmholtz free-energy surface $F(T,V)$, as a function of the temperature T and the crystal volume V, is considered in the adiabatic approximation

$$F(T,V) = F^{\mathrm{vib}}(T,V) + F^{\mathrm{el}}(T,V) + F^{\mathrm{mag}}(T,V), \qquad (1)$$

that treats the vibrational F^{vib}, the electronic F^{el} (including the energy of the static lattice), and the magnetic F^{mag} contribution separately. For iron, the adiabatic approximation is well justified since the underlying mechanisms, i.e., phonon, electron, and magnon excitations, reside on different time scales.[18] The validity of the adiabatic approximation is further supported by recent explicit *ab initio* calculations of the magnon-phonon coupling in iron.[19]

To calculate F^{vib}, F^{el}, and F^{mag}, we employ the VASP (Ref. 20) package using the projector augmented wave method[21] within the generalized gradient approximation (Perdew-Burke-Ernzerhof parametrization[22]).[23] Anharmonic contributions are expected to be small (a few meV) and will, therefore, not be considered in this study.[24] The contributions of F^{vib} and F^{el} are calculated within the quasiharmonic approximation and finite-temperature DFT,[25] respectively, as discussed in detail in Ref. 5. As the first step, we have, therefore, calculated the phonon dispersion of ferromagnetic bcc iron, which serves as an input to the partition function needed for computing F^{vib}. The comparison with the experimental phonon spectrum shows a good agreement (Fig. 1).[29] The resulting combined vibronic and electronic free energy ($F^{\mathrm{vib}}+F^{\mathrm{el}}$) is shown in Fig. 2 (black line) and compared to CALPHAD data. Clearly, the deviation between *ab initio* ($F^{\mathrm{vib}}+F^{\mathrm{el}}$) and CALPHAD data rapidly increases with temperature. For instance, at 1200 K, which corresponds to the experimental bcc to fcc transition temperature, the difference is $\approx$45 meV. An even more sensitive physical quantity

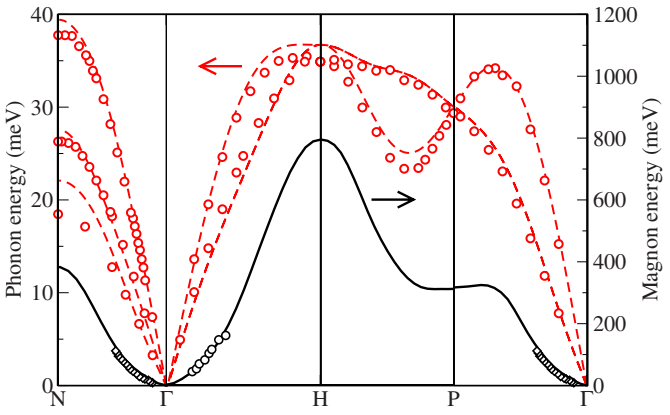

FIG. 1. (Color online) *Ab initio* phonon (dashed line, left axis, at 300 K) and magnon (solid line, right axis, at 0 K) spectrum of ferromagnetic bcc iron. The results are, respectively, compared with available neutron-scattering data (Refs. 26–28).

that allows the checking of the predictive accuracy of the *ab initio* calculations is the heat capacity C_P, which is the second derivative of the free-energy surface with respect to temperature. Figure 3 shows that the combined vibronic and electronic heat capacity agrees well with experimental data only up to ≈300 K, which is in agreement with Ref. 33. At higher temperatures, however, Fig. 3 clearly reveals that it cannot account for the rapid increase in the experimental heat capacity. It is, therefore, obvious that an accurate determination of the free-energy contribution from magnetic excitations is crucial.

We derive the magnetic free energy F^{mag} from the solution of the Heisenberg Hamiltonian within many-body theory in the mean-field (MF) approximation and in the random-phase approximation (RPA). The Heisenberg Hamiltonian is entirely determined by the spin quantum number S and the coefficients J_{ij}, which describe the magnetic exchange coupling between magnetic moments at atomic sites i and j. The spin quantum number S is connected to the local magnetic moment M_0 by $M_0=g\mu_B S$, with the Landé factor g and the Bohr magneton μ_B. For iron, M_0 is almost entirely determined by the strongly localized $3d$ electrons and is, therefore, given by the total magnetization scaled by the number of atoms and $g\approx 2$. Our $T=0$ K result of the total magnetic moment gives

$$M_0 \approx 2.2\mu_B \rightarrow S \approx 1.1. \tag{2}$$

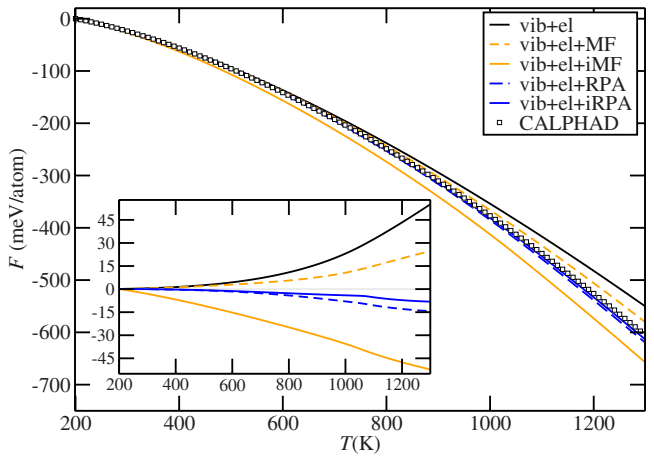

FIG. 2. (Color online) *Ab initio* free energy F at zero pressure as a function of temperature T, including various combinations of the vibrational (vib), electronic (el), and magnetic contribution. The latter has been calculated within the MF, iMF, RPA, and iRPA. The CALPHAD data has been obtained with the THERMOCALC program and the SGTE unary database (Ref. 30). Inset. The CALPHAD data are taken as the reference at each temperature.

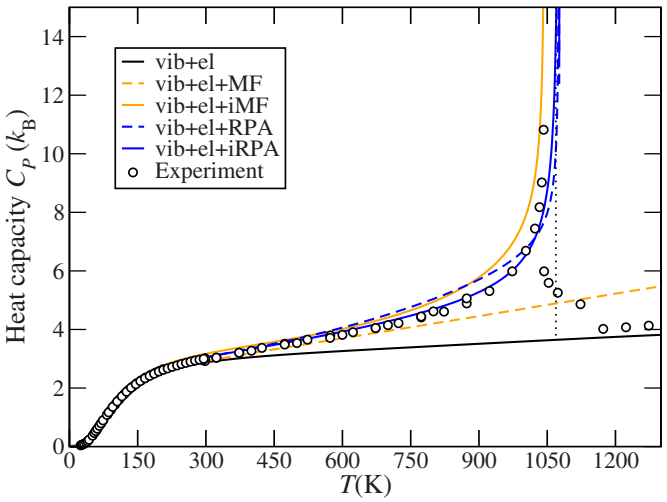

FIG. 3. (Color online) Heat capacity C_P in units of the Boltzmann constant k_B at zero pressure P as a function of temperature T, including the various contributions as specified in Fig. 2. The experimental data are from Refs. 31 and 32.

For extracting the magnetic exchange coefficients J_{ij}, we use the frozen magnon approach,[9] employing the generalized Bloch theorem.[34] In this approach, the DFT energy difference between different spin spirals is calculated in reciprocal space. In order to estimate the accuracy of our computed coefficients, we calculate the magnon energies $\omega_{\mathbf{q}}$ at special reciprocal vectors $\mathbf{q}$ using $\omega_{\mathbf{q}}=4(J_{\mathbf{q}=0}-J_{\mathbf{q}})/M_0=4\Delta E_{\mathbf{q}}/M_0$,[7,9,15] where the $J_{\mathbf{q}}$ are the exchange coefficients at the corresponding $\mathbf{q}$ that are related to J_{ij} via Fourier transformation and $\Delta E_{\mathbf{q}}$ is the *ab initio* calculated energy difference with respect to the ferromagnetic ground state. The results are shown in Fig. 1 and reveal an excellent agreement between the calculated magnon spectrum (solid black line) and corresponding experimental data.

Using our computed spin quantum number and exchange coefficients, we calculate the internal energy $U^{\mathrm{mag}}(T)$, from which F^{mag} can be obtained by integration (see Ref. 35). Within MF, U^{mag} is simply proportional to the square of the magnetization, which in turn is given by a Brillouin function (see Fig. 4).[35] The obtained MF free energy and heat capacity are shown in Figs. 2 and 3 (orange dashed lines), respectively. Up to ≈700 K, both quantities are reasonably improved with respect to the pure vibrational and electronic contributions, but MF fails to reproduce the singularity of the heat capacity at the predicted Curie temperature $T_C^{\mathrm{MF}}=2J_0/(3k_B)=1521$ K, where k_B is the Boltzmann constant. Furthermore, the calculated T_C^{MF} is in fact 1.5 times higher

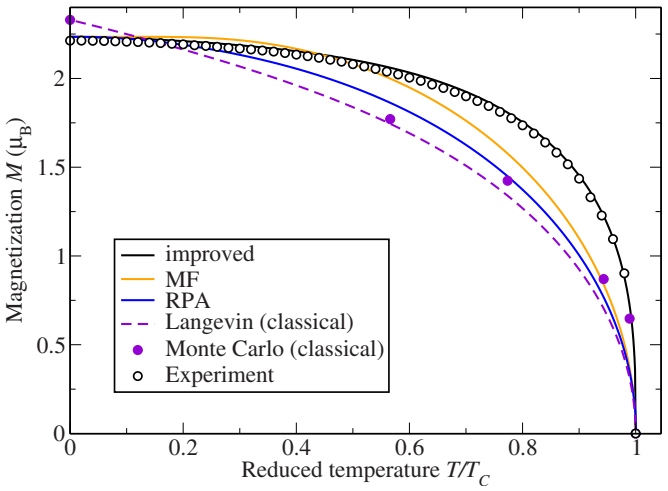

FIG. 4. (Color online) Comparison of several theoretical approximations for the magnetization $M(T)=M_0m(T)$ in comparison with experimental data (Ref. 36) and Monte Carlo calculations (Ref. 10). The results are plotted as a function of the reduced temperature T/T_C.

than the experimental $T_C^{\mathrm{exp}}=1044$ K. Such a high overestimation of the Curie temperature is a known deficiency of the MF approximation.[15] The inability to reproduce the singularity is related to the poor description of the temperature-dependent magnetization within MF, as will be discussed later.

The RPA is an approximation which is known to give more accurate Curie temperatures.[11,14,15] Within RPA $T_C^{\mathrm{RPA}}=2[\Sigma_{\mathbf{q}}1/(J_0-J_{\mathbf{q}})]^{-1}/(3k_B)$, we obtain a value which is much closer to the experiment $T_C^{\mathrm{RPA}}=1082$ K. However, deriving an expression for the internal energy of a spin system with $S>1/2$ [as for bcc iron, see Eq. (2)] is much more challenging[37] than for a $S=1/2$ system, where the expression for the longitudinal correlation function has already been derived consistently.[35] In order to make use of the RPA despite these complications, we apply the following procedure: We start with the known self-consistent expression for the magnetization $M(T)$ of the $S=1/2$ system and introduce a renormalization factor γ for the exchange coefficients in such a way that T_C^{RPA} is obtained as $M(T)\rightarrow 0$. The renormalized magnetization obtained with this approach is given by

$$m(T)=\left\{1+\frac{2}{N}\sum_{\mathbf{q}}\exp[2\beta m(T)\gamma(J_0-J_{\mathbf{q}})]\right\}^{-1}, \qquad (3)$$

where $m(T)=M(T)/M_0$, $\beta=1/k_BT$, and $\gamma=\frac{2}{3}$.

Starting from the $S=1/2$ expression for the internal energy and introducing the γ factor for the exchange coefficients analogously to Eq. (3), we end up with

$$U^{\mathrm{mag}}(T)=U_{T=0}^{\mathrm{mag}}+\frac{M_0}{2}\sum_{\mathbf{q}}\frac{2m(T)[m(T)+1]\gamma[J_0-J_{\mathbf{q}}]}{\exp[2\beta m(T)\gamma(J_0-J_{\mathbf{q}})]-1}. \qquad (4)$$

Using this theory, the divergence in the heat capacity due to the second-order phase transition from the ferromagnetic to the paramagnetic phase at T_C is now correctly reproduced (see Fig. 3). Above T_C, $U^{\mathrm{mag}}=0$ within both MF and RPA, which, in contrast to experiment, gives vanishing contribution to the heat capacity C_P. Both approximations, MF and RPA, are not capable to describe the region above T_C because these approximations do not capture the local magnetic order dominating in this temperature region. This restriction does not, however, affect the absolute free energy as strongly as it affects its second derivative, which is the heat capacity. Figure 2 indeed reveals that the integrated RPA free energy deviates from the CALPHAD data by less than 15 meV at 1200 K. In order to figure out the origin of the remaining differences between *ab initio* and experimental data, we investigate whether these differences can be decreased by using an improved description of the temperature-dependent magnetization $m(T)$. The RPA relation between the magnetic internal energy $U^{\mathrm{mag}}(T)$ and the magnetization $m(T)$ follows from Eq. (4). In Fig. 4, we show the magnetization curves obtained with MF and RPA and compare them with experimental results. The classical solution found by Monte Carlo simulations[10] and a Langevin function are also shown for comparison. Clearly, both approximations, MF and RPA, are not able to accurately reproduce the experimental data. Hence, in order to improve their description of the free energy and heat capacity, we use an improved magnetization curve m^{imp} for ferromagnetic bcc iron,

$$m^{\mathrm{imp}}(T)=[1-s(T/T_C)^{3/2}-(1-s)(T/T_C)^4]^{1/3}, \qquad (5)$$

that fulfills Bloch's famous $T^{3/2}$ law for low temperatures and was empirically derived from a detailed analysis of the corresponding experimental data for several ferromagnetic systems.[38] The only free parameter s in Eq. (5) can be calculated using *ab initio* input.[39] The obtained shape of the magnetization describes perfectly the experimental data, as shown in Fig. 4 (black line).[40]

The improved magnetization [given by Eq. (5)] is now used as input to U^{mag} in MF and RPA [labeled as improved mean field (iMF) and improved random-phase approximation (iRPA)]. For the improved MF,[41] the calculated heat capacity (orange solid line in Fig. 3) shows the correct qualitative behavior and comes significantly closer to experiment. For the free energy, however, the deviation from experiment becomes more pronounced and even undergoes a sign reversal (Fig. 2). Therefore, we conclude that even an employment of the improved temperature-dependent magnetization is not sufficient to account for the magnetic contribution to the free energy within MF approximation. In contrast, a noticeable improvement of both C_P and F is obtained for the improved RPA. The experimental heat capacity is now nearly perfectly predicted up to T_C. The difference between the theoretical integrated free energy with a magnetic contribution calculated with iRPA and the corresponding CALPHAD data decreases to less than 10 meV at 1200 K.

In conclusion, by generalizing the $S=1/2$ RPA theory of the Heisenberg model, we were able to calculate the magnetic contribution to the Helmholtz free energy of a system with $S>1/2$. Combining this approach with highly converged vibrational and electronic contributions, all relevant parts of the free energy of magnetic materials can be deter-

mined solely on the basis of *ab initio* input. Applying this approach to ferromagnetic bcc iron, we find that DFT (using the generalized gradient approximation Perdew-Burke-Ernzerhof parametrization) allows an (surprisingly) accurate description of the free energy and the heat capacity in the temperature range, where it is known to be thermodynamically stable (from 0 to 1200 K). We expect that this approach provides a similar accuracy for other ferromagnetic materials, which allows the accurate prediction of their thermodynamic properties from first principles.

Financial support of the collaborative research center 761 of the Deutsche Forschungsgemeinschaft is gratefully acknowledged.

*koermann@mpie.de

[1] L. Kaufman and H. Bernstein, *Computer Calculation of Phase Diagrams* (Academic, New York, 1970).
[2] N. Saunders and A. P. Miodownik, *Calphad (Calculation of Phase Diagrams): A Comprehensive Guide* (Pergamon, Oxford, 1998).
[3] P. E. A. Turchi, I. A. Abrikosov, B. Burton, S. G. Fries, G. Grimvall, L. Kaufmann, P. Korzhavyi, V. R. Manga, M. Ohno, A. Pisch, A. Scott, and W. Zhang, CALPHAD: Comput. Coupling Phase Diagrams Thermochem. **31**, 4 (2007).
[4] P. Souvatzis and O. Eriksson, Phys. Rev. B **77**, 024110 (2008).
[5] B. Grabowski, T. Hickel, and J. Neugebauer, Phys. Rev. B **76**, 024309 (2007).
[6] W. Nolting, A. Vega, and T. Fauster, Z. Phys. B: Condens. Matter **96**, 357 (1995).
[7] J. Kübler, J. Phys.: Condens. Matter **18**, 9795 (2006).
[8] J. Kübler, G. H. Fecher, and C. Felser, Phys. Rev. B **76**, 024414 (2007).
[9] S. V. Halilov, A. Y. Perlov, P. M. Oppeneer, and H. Eschrig, Europhys. Lett. **39**, 91 (1997).
[10] N. M. Rosengaard and B. Johansson, Phys. Rev. B **55**, 14975 (1997).
[11] J. Rusz, L. Bergqvist, J. Kudrnovský, and I. Turek, Phys. Rev. B **73**, 214412 (2006).
[12] M. Ležaić, P. Mavropoulos, and S. Blügel, Appl. Phys. Lett. **90**, 082504 (2007).
[13] A. V. Ruban, S. Khmelevskyi, P. Mohn, and B. Johansson, Phys. Rev. B **75**, 054402 (2007).
[14] G. Y. Gao, K. L. Yao, E. Şaşioğlu, L. M. Sandratskii, Z. L. Liu, and J. L. Jiang, Phys. Rev. B **75**, 174442 (2007).
[15] M. Pajda, J. Kudrnovsky, I. Turek, V. Drchal, and P. Bruno, Phys. Rev. B **64**, 174402 (2001).
[16] L. Kaufman, E. V. Clougherty, and R. J. Weiss, Acta Metall. **11**, 323 (1963).
[17] H. Hasegawa and D. G. Pettifor, Phys. Rev. Lett. **50**, 130 (1983).
[18] D. C. Wallace, *Thermodynamics of Crystals* (Dover, New York, 1998).
[19] R. F. Sabiryanov and S. S. Jaswal, Phys. Rev. Lett. **83**, 2062 (1999).
[20] G. Kresse and J. Furthmüller, Phys. Rev. B **54**, 11169 (1996).
[21] P. E. Blöchl, Phys. Rev. B **50**, 17953 (1994).
[22] J. P. Perdew, K. Burke, and M. Ernzerhof, Phys. Rev. Lett. **77**, 3865 (1996).
[23] The following converged parameters have been used. Vibrational part: 54 atom supercell; ≈27000 **k**-points atom (kp·a); plane-wave cutoff energy E_{cut}=340 eV. Electronic part: ≈40000 kp·a; E_{cut}=340 eV. Magnetic part: ≈7000 kp·a; E_{cut}=400 eV; ≈3000 **q**-points for the magnetic integration in Eqs. (3) and (4).
[24] M. Forsblom, N. Sandberg, and G. Grimvall, Phys. Rev. B **69**, 165106 (2004).
[25] N. D. Mermin, Phys. Rev. **137**, A1441 (1965).
[26] J. Lynn, Phys. Rev. B **11**, 2624 (1975).
[27] C. Loong, J. Carpenter, J. Lynn, R. Robinson, and H. Mook, J. Appl. Phys. **55**, 1895 (1984).
[28] *Metals: Phonon States, Electron States and Fermi Surfaces*, Landolt-Börnstein, New Series, Group III, Vol. 13 (Springer-Verlag, Berlin, 1981).
[29] The small difference between experimental and our theoretical phonon energies of <5 meV is due to the exchange-correlation functional. Using a Born-von Kármán fit for the experimental as well as for the theoretical phonon dispersions we estimate the difference in the free energy to be around 5 meV/atom at 1300 K.
[30] A. F. Guillemet and P. Gustafson, High Temp. - High Press. **16**, 591 (1985).
[31] D. C. Wallace, P. H. Sidles, and G. C. Danielson, J. Appl. Phys. **31**, 168 (1960).
[32] Y. S. Touloukian and E. H. Buyco, *Thermophysical Properties of Matter* (IFI/Plenum, New York-Washington, 1970), Vol. 4.
[33] X. Sha and R. E. Cohen, Phys. Rev. B **73**, 104303 (2006).
[34] L. M. Sandratskii, Adv. Phys. **47**, 91 (1998).
[35] W. Nolting, *Grundkurs Theoretische Physik 7* (Springer-Verlag, Berlin, 2005).
[36] J. Crangle and G. M. Goodman, Proc. R. Soc. London, Ser. A **321**, 477 (1971).
[37] R. A. Tahir-Kheli, Phys. Rev. **159**, 439 (1967).
[38] M. D. Kuz'min, Phys. Rev. Lett. **94**, 107204 (2005).
[39] M. D. Kuz'min, M. Richter, and A. N. Yaresko, Phys. Rev. B **73**, 100401(R) (2006).
[40] The calculated s=0.41 is close to the empirical value s=0.35 found by fitting Eq. (5) to experimental data (Ref. 38). The *ab initio* values used to calculate the theoretical s are: The ground state magnetization M_0=2.23 μ_B; the spin wave stiffness D=249 meV Å^2 obtained from the low excitation spectrum $\omega(\mathbf{q}\rightarrow 0)\approx Dq^2$ (which agrees with other theoretical works (Ref. 15); T_C^{RPA}=1082 K.
[41] In case of MF, T_C^{exp} is used since MF highly overestimates the Curie temperature.